

# The Structural Basis of Repertoire Shift in an Immune Response to Phosphocholine

By McKay Brown,\* Maria A. Schumacher,† Gregory D. Wiens,\* Richard G. Brennan,§ and Marvin B. Rittenberg\*

From the \*Department of Molecular Microbiology and Immunology, †The Vollum Institute, and the

§Department of Biochemistry and Molecular Biology, Oregon Health Sciences University, Portland, Oregon 97201-3098

## Abstract

The immune response to phosphocholine (PC)-protein is characterized by a shift in antibody repertoire as the response progresses. This change in expressed gene combinations is accompanied by a shift in fine specificity toward the carrier, resulting in high affinity to PC-protein. The somatically mutated memory hybridoma, M3C65, possesses high affinity for PC-protein and the phenyl-hapten analogue, *p*-nitrophenyl phosphocholine (NPPC). Affinity measurements using related PC-phenyl analogues, including peptides of varying lengths, demonstrate that carrier determinants contribute to binding affinity and that somatic mutations alter this recognition. The crystal structure of an M3C65-NPPC complex at 2.35-Å resolution allows evaluation of the three light chain mutations that confer high-affinity binding to NPPC. Only one of the mutations involves a contact residue, whereas the other two have indirect effects on the shape of the combining site. Comparison of the M3C65 structure to that of T15, an antibody dominating the primary response, provides clear structural evidence for the role of carrier determinants in promoting repertoire shift. These two antibodies express unrelated variable region heavy and light chain genes and represent a classic example of the effect of repertoire shift on maturation of the immune response.

Key words: immunoglobulin • somatic mutation • X-ray crystallography • antibody affinity • affinity maturation

## Introduction

Affinity maturation of serum antibodies occurs during the immune response to T cell-dependent antigens (1) and can be critical for protective immunity. In many antibody responses, much of the diversity exhibited by secondary and memory antibody populations is provided by somatic mutation of primary gene combinations (2–5). However, another level of diversity can also be provided by recruitment of new germline VH and VL genes during the response, termed repertoire shift (6). These new gene combinations are frequently modified by mutation, providing high affinity for the immunogen (4, 6–8). The molecular basis of this selective process is not entirely clear, but may depend in part on a shift in specificity toward recognition of the hapten plus carrier determinants.

M. Brown and M.A. Schumacher contributed equally to this work.

Address correspondence to McKay Brown, Department of Molecular Microbiology and Immunology, L220, Oregon Health Sciences University, 3181 S.W. Sam Jackson Park Rd., Portland, OR 97201. Phone: 503-494-7718; Fax: 503-494-6862; E-mail: nuttm@ohsu.edu

The antibody response to phosphocholine (PC)<sup>1</sup> is biologically interesting because of the frequent expression of PC on pathogenic bacteria and nematodes where the haptenic epitope is coupled to a variety of carrier structures, including carbohydrates and proteins (9–11). The murine response to PC-protein is a well-characterized model system used to study the shift in specificity to include the carrier as the immune response progresses (7, 12–15). After immunization with PC coupled to KLH via a diazophenyl linker, the antibody population specific for PC at the onset of the primary response (group I antibodies) shifts to one that includes the carrier as part of a more complex epitope. Thus the response matures, evolving toward a population that has a strong requirement for PC in the context of the nitrophenyl linker (group II antibodies). The emergent group II antibody population requires recruitment and ex-

<sup>1</sup>Abbreviations used in this paper: PC, phosphocholine; sFv, single-chain Fv fragment; MR, molecular replacement.

pansion of B cell clones expressing novel V gene combinations rarely seen in the primary response (7). The expansion and eventual dominance by a minor component of the initial antibody repertoire points to the importance of carrier determinants in selecting and stimulating lymphocytes of the group II phenotype that predominate in the memory pool.

We have shown previously that somatic mutation in a prototype group II hybridoma, M3C65, results in a dramatic increase in affinity for antigen. High affinity for *p*-nitrophenyl phosphocholine (NPPC), a hapten that mimics the diazophenyl linkage between PC and protein, is attributable to mutations at three positions in CDR2 of the M3C65  $\lambda 1$  L chain (16). Accumulation of replacement mutations at these key positions in the L chain occurs repeatedly in B cells undergoing affinity maturation in response to PC-KLH (17).

In this study, we use crystallographic and affinity analysis to reveal the molecular basis for the repertoire shift that occurs after immunization with PC-KLH. We determine the intrinsic affinity of M3C65 in its mutated and germline forms for compounds representing various portions of the carrier protein coupled to PC. We also solved the crystal structure of the single-chain Fv (sFv) of this antibody complexed to NPPC. The M3C65 combining site has an unusual requirement for direct interaction of the LCDR2 with NPPC, a finding that is rare for binding of small haptens molecules (18). The structure of the complex provides a stereochemical basis for emergence of group II dominance in a secondary response, and allows evaluation of the direct and indirect effects of L chain modification by somatic mutation in generating high affinity in the M3C65 hybridoma.

## Materials and Methods

**Synthesis and Expression of M3C65 sFv.** cDNA copies of the VH and VL genes of the hybridoma M3C65 (16) were synthesized from mRNA using random hexamer primers (Amersham Pharmacia Biotech). PCR amplification was carried out using a primer for the 5' portion of  $V\lambda 1$  (5'-agatcgcatccatggGACA-GGCTGTTGTGACTCATGGAA-3') and a primer for the 3' portion of  $J\lambda 1$  plus the 5' part of the (Gly<sub>4</sub>Ser)<sub>3</sub> linker (5'-cggacccacc-accggccgagccaccgcaccACCTAGGACAGTCAGTTGGT-3'). Amplification of the VH M141/D/JH3 gene was carried out using a primer for the 3' part of the linker plus the 5' VH (5'-tcggcgttgtggccggaggcgatctCAGGTGCAGCTGAAGGAGTC AG-3') and a primer for the 3' end of JH3 plus two stop codons and an NcoI site (5'-agatcgcatccatggttatcaTGCAGAGACAGTGACCAGAGTCCC-3'). NcoI sites are underlined, and V region coding sequences are capitalized. The VL and VH genes were joined by PCR with the linker (Gly<sub>4</sub>Ser)<sub>3</sub> in the order VL-linker-VH. The amplified sFv DNA was ligated into the NcoI site of the pET3d vector (Novagen), sequenced, and transformed into *Escherichia coli* Bl21(DE3). DNA sequencing of clone 2-1.2 showed that the deduced protein sequence was identical to the M3C65 hybridoma. The induced protein sFv inclusions (24.9 kD) were denatured and refolded as described (19). Renatured sFv fragments were purified by affinity chro-

matography on PC-sepharose as described for intact antibody (12).

**Transfект Antibodies and  $K_a$  Determination.** Antibodies expressing mutations at  $\lambda$  L chain positions 52, 53, or 55 produced by site-directed mutagenesis and the method for determination of binding constants by fluorescence quenching have been described (16). Stable transfectants cotransfected with the M3C65 H chain and the various mutant L chain constructs were made in the SP2/0 cell line and purified as described previously (16). The synthesis and structure of monoconjugates of PC coupled to tyrosine, histidine, and the Gly-Tyr-Ala tripeptide have been described; PC is coupled to Tyr on the tripeptide (20). These compounds were provided by Drs. D. Peyton, E. Barbar, and H. Moulton (Portland State University, Portland, OR). A 15-amino acid peptide, acetylated at the NH<sub>2</sub> terminus (Peptide Express), was designed to contain one haptene site and to have  $\alpha$ -helical secondary structure (21). The peptide, Ser-Asp-Ala-Leu-Ala-Glu-Met-Tyr-Glu-Leu-Met-Ala-Val-Asp-Gly, was coupled to PC at the Tyr residue as described previously (22). PC-histone was coupled by the same method and has a PC/protein ratio of 2:1.

**Crystallization of M3C65 sFv Complexed to NPPC.** The purified sFv at 400  $\mu$ g/ml was dialyzed against 20 mM Tris, pH 7.6, concentrated to 5.6 mg/ml, and NPPC was added to a final concentration of 2 mM. Crystals were grown at room temperature by vapor diffusion from a reservoir buffer that contained 1.5 M NaH<sub>2</sub>PO<sub>4</sub>/K<sub>2</sub>HPO<sub>4</sub>, pH 6.5, and 0.1 M Hepes buffer (GIBCO BRL). The crystals are orthorhombic, take the space group P2<sub>1</sub>2<sub>1</sub>2<sub>1</sub> ( $a = 130.5 \text{ \AA}$ ,  $b = 35.9 \text{ \AA}$ ,  $c = 50.5 \text{ \AA}$ ), and contain one monomer in the asymmetric unit.

**Data Collection and Structure Solution.** X-ray intensity data were collected at room temperature using a RAXIS IV (Rigaku) imaging plate system and a Rigaku RU300 rotating anode X-ray generator equipped with double-focusing mirrors and operating at 50 kV and 100 mA. Data were processed with BIOTEX (Molecular Structure Corporation, Inc.). The structure was solved by molecular replacement (MR) using data from 8.0- to 4.0- $\text{\AA}$  resolution and the  $\lambda 1$  L chain from antibody HC19 (23), 1GIG, as the search model. The MR was carried out using EPMR (24), which resulted in a solution with a correlation coefficient of 0.372. Search models using structures of several antibody H chains failed to produce a solution. Rigid body refinement of the L chain using TNT (25), using data from 10.0 to 3.0  $\text{\AA}$ , reduced the R factor to 44.6%. Phases from this partial structure were used to calculate an electron density map that revealed some interpretable density for the H chain. The D1.3 H chain (26), 1VFA, was then manually rotated into the density, and rigid body refinement was carried out. This reduced the R factor to 35.6%, at which point the correct side chains were substituted in the H chain. Positional (xyz) refinement, using data from 10.0 to 2.8  $\text{\AA}$ , was then initiated, and reduced the R factor to 22.9%. The resulting electron density map revealed very clear density for the NPPC hapten, which was then included, and the resulting model was refined via xyz, and subsequently via positional and thermal parameter (xyzb) refinement. xyzb refinement was carried out initially using data from 10.0- to 2.6- $\text{\AA}$  resolution. The final refinement included data extending from 10.0- to 2.35- $\text{\AA}$  resolution. The current structure includes residues 1-109 of the L chain, 1-112 of the H chain, the NPPC molecule, and 88 solvent molecules. PROCHECK analysis (27) revealed 97.9% of residues in allowed regions (78% in most favored), and 2.1% in generously allowed regions. See Table II for selected crystallographic refinement statistics. Coordinates have been deposited in the Protein Data Bank with accession code 1DL7.

## Results

**Affinity of M3C65 Wild-Type and Mutant Antibodies.** The M3C65 hybridoma antibody ( $\gamma$ 2b,  $\lambda$ 1) is a member of a set of clonally related antibodies produced in a secondary response to PC-protein. High affinity for the hapten analogue NPPC is attributable to mutations at positions 52, 53, and 55 in CDR2 of the  $\lambda$ 1 L chain (16). Mutations at these key positions occur repeatedly in M3C65 clonal relatives, as well as in unrelated  $\lambda$ -bearing anti-PC protein hybridomas, indicating that LCDR2 replacements are vital to expansion and selection of these memory antibodies (16, 17). To assess whether the hapten-carrier linkage beyond the diazophenyl moiety forms part of the immunogenic structure of PC-KLH, we have analyzed binding to a number of structures representing distinct carrier epitopes. We also determined whether these structures are recognized differently as mutations accumulate. A comparison was made of the affinity of antibody constructs expressing zero (germline), one, or two mutations with the binding of M3C65, which contains all three pertinent mutations in LCDR2. The sequences of the H and L chain V regions and the positions of mutations are indicated in Fig. 1. The PC ligands used to measure affinity by fluorescence quenching are shown in Fig. 2.

Diazophenyl links preferentially to tyrosine or histidine residues in proteins (28). Because both KLH isoforms contain multiple tyrosine and histidine residues (29), both amino acids are likely to be haptenated during conjugation of PC to KLH via a diazophenyl linkage. To analyze the contribution of a single amino acid linked via diazophenyl to PC, we compared the affinity for PC-tyrosine or PC-

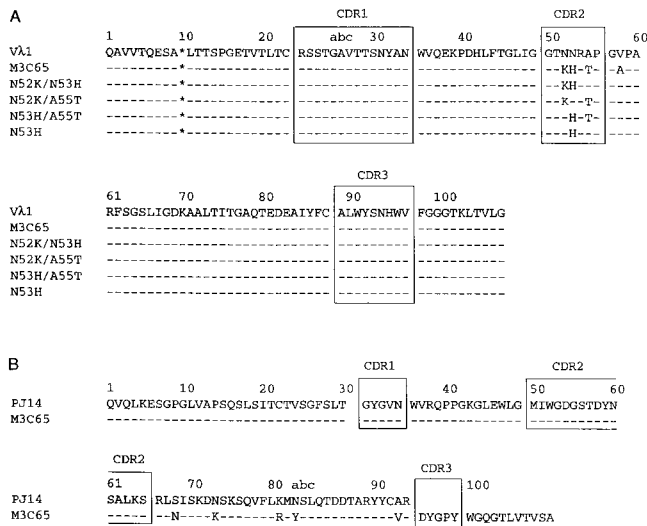


**Figure 1.** Amino acid sequences of the M3C65 hybridoma antibody and transfected mutant antibodies. The numbering is according to Kabat et al. (80). Dashes indicate identity with the germline sequence. The sequences of the VH and VL regions of the M3C65 hybridoma are identical to the sFv fragment expressed in *E. coli*. (A) Vλ1 sequences. There is a deletion of framework 1 residue 10 in Vλ sequences (80), indicated by \*. (B) VH sequences. M3C65 uses the germline PJ14 (Q52 family) and JH3 gene segments (16).

histidine to the affinity for NPPC in antibodies expressing germline or mutated L chains. As shown in Table I, the relative affinity for ligand of antibody expressing the unmutated L chain is PC-histidine  $\geq$  PC-tyrosine > NPPC, with the affinity for PC-histidine about ten times that of the affinity for NPPC. Although the affinity for NPPC increased as mutations accumulated in the L chain, all the mutant antibodies had higher affinity for PC-tyrosine and PC-histidine compared with antibody expressing germline L chain. It is noteworthy that ligand recognition shifts toward PC-tyrosine with the accumulation of mutations in the M3C65 antibody. Thus, binding to PC-tyrosine or PC-histidine allows for detection of changes in fine specificity, with the affinity of the mutated M3C65 antibody for PC-tyrosine being fivefold greater than for PC-histidine. These results demonstrate that carrier determinants, as represented by tyrosine and histidine, contribute to binding, and that somatic mutation can modulate carrier recognition.

How much of the PC-protein carrier provides determinants recognized by group II antibodies? Previous experiments involving inhibition of binding of M3C65 to PC-

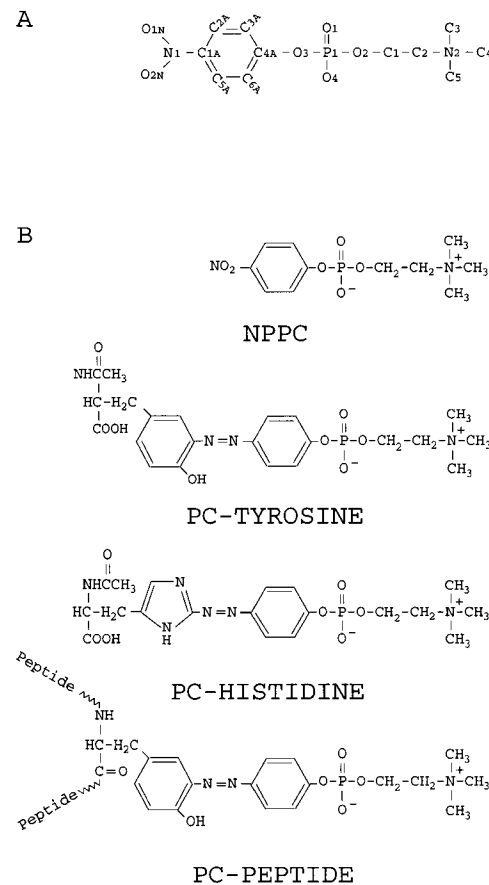


**Figure 2.** (A) Atom labeling for the hapten NPPC. (B) Chemical structure of PC ligands used in affinity determinations. The PC-peptide sequence is Gly-Tyr-Ala with PC coupled to the Tyr residue, or Ser-Asp-Ala-Leu-Ala-Glu-Met-Tyr-Glu-Leu-Met-Ala-Val-Asp-Gly with PC coupled to the Tyr residue.

**Table I.** Binding Constants Determined by Fluorescence Quenching

λ1 CDR2 residues									
Germline	52 N	53 N	55 A	NPPC	PC–tyrosine	PC–histidine	PC–GYA (3 residues)	PC–peptide (15 residues)	PC–histone
$K_a \times 10^6 (M^{-1})^*$									
M3C65	K	H	T	3.1 (0.2) <sup>†</sup>	51.1 (0.5)	10.8 (2.8)	5.5 (2.0)	339.2 (72.8)	120.8 (6.0)
MC365 sFv	K	H	T	2.8 (0.2)	53.2 (0.2)	15.0 (0.3)	7.5 (0.5)	ND	78.9 (32.7)
Mutants	K	H	–	2.6 (1.0)	38.7 (0.1)	34.5 (13.2)	29.2 (4.9)	373.9 (64.1)	78.9 (5.1)
	K	–	T <sup>§</sup>	0.2 (0.1)	7.5 (0.6)	38.1 (10.3)	10.1 (0.6)	ND	ND
	–	H	T	0.7 (0.4)	23.2 (5.6)	44.8 (10.2)	37.5 (14.1)	ND	ND
	–	H	–	0.03 (0.01)	0.2 (0.1)	1.8 (0.1)	3.2 (1.0)	229.6 (30.1)	104.7 (6.0)
Germline	–	–	–	0.03 (0.00)	0.1 (0.03)	0.4 (0.2)	2.9 (0.4)	Not detectable	0.5 (0.1)

\*Affinity constants ( $K_a$ ) were determined by fluorescence quenching at 25°C.

†Values in parentheses are SDs of two to four determinations.

<sup>§</sup>This combination of replacement mutations has not been observed in natural group II hybridomas.

protein in an ELISA showed that  $\sim 10^5$  times more NPPC than PC–BSA was required to reduce binding by 50% (16). Is the superior inhibitory capacity of PC–protein due solely to the effects of avidity, or does effective binding correlate with an increase in size of the carrier? To answer these questions, we determined the intrinsic affinity of antibody for PC coupled to carriers of varying sizes. The tripeptide and the 15-amino acid peptide each have only one tyrosine (and no histidine) in the sequence, and are monosubstituted with PC (discussed in Materials and Methods), whereas the histones have multiple tyrosine and histidine residues (30). The results in Table I show that affinity of antibody expressing germline λ1 for the PC–GYA tripeptide is higher than for PC–tyrosine, PC–histidine, or PC–histone. These findings indicate that neither size nor avidity alone provides the advantage, but that qualitative characteristics of each individual carrier can be critical. After the introduction of the single mutation at position 53, binding to the monosubstituted 15-amino acid PC–peptide and to PC–histone is at levels near or equal to the fully mutated antibody. Thus, it appears that an increase in size of the carrier would beneficially affect binding to germline-encoded antibodies up to a certain point (PC–GYA > PC–histidine > NPPC), but a further increase in size represented by the protein conjugate, PC–histone, confers little affinity advantage until mutation occurs.

The cumulative effects of somatic mutation on binding of small haptens in several systems indicate that high affinity can result from incremental improvements as mutations accumulate (31, 32). In M3C65, acquisition of high affinity for NPPC, PC–tyrosine, or PC–histidine by introduction of L chain mutations follows a similar pattern (Table I). In contrast, introduction of a single mutation at LCDR2 position 53 accounts for high-affinity binding of the monosubstituted 15-amino acid PC–peptide and results in a 200-fold increase in affinity for PC–histone. Thus, binding to

the haptenic compounds mimics the stepwise acquisition of high affinity for small haptens seen with other antibodies, whereas high affinity to the larger PC–carrier structures may result from a single substitution. Production of a high-affinity antibody by a single mutation emphasizes the adaptive potential of the group II combining site (33). The surprising difference in the effect of mutation on binding of the various PC-containing compounds raises a cautionary note concerning the extrapolation of antihapten binding results to the *in vivo* situation, where the complete hapten conjugate may be the structure relevant to shaping of the immune repertoire. In addition, as demonstrated here and by others, somatic mutation not only increases affinity for hapten, but may also shift antigenic specificity (34–36).

**Structure Determination and Overall Structure of the M3C65 sFv–NPPC Complex.** To determine the molecular basis of PC–carrier recognition and the contribution of somatic mutations, the crystal structure of an M3C65 sFv fragment complexed with NPPC was determined at a resolution of 2.35 Å (atom labeling of NPPC shown in Fig. 2 A). The sFv fragment of M3C65 was used for crystallographic analysis because the sFv binding data were in good agreement with that of intact antibody (Table I). Attempts to analyze the sFv fragment bound to the higher-affinity ligand, PC–tyrosine, were unsuccessful because the complex did not yield data-quality crystals. The crystallographic data collection and refinement statistics for the sFv–NPPC complex are shown in Table II.

The combining site of M3C65 is a long narrow groove,  $\sim 15$  Å long by 5 Å wide by 7 Å deep, created by residues from LCDR1, LCDR2, LCDR3, HCDR2, and HCDR3 (Fig. 3). The binding pocket is unusual in that it is enclosed at one end by LCDR2 residue Thr55, which seals off the *p*-nitrophenyl group of the hapten from solvent. Contact with LCDR2 is rare in antibodies recognizing small haptens (18), but has been seen in the anti-DNP antibody

**Table II.** Data Collection and Refinement Statistics

Resolution range (Å)	10.0–2.35
No. of reflections	8,983
No. of measurements	47,930
Completeness (%)	84
I/(σ)I	8.5
Rsym*	7.3
Data for highest shell (2.42 to 2.35 Å)	
Completeness (%)	47
I/(σ)I	1.5
Rsym*	26.5
R factor (%)‡	19.1
R free (%)§	26.5
No. of atoms	1,680
No. of solvent molecules	88
Rms deviations	
Bond lengths (Å)	0.014
Bond angles (°)	1.901
B factors (Å²)	3.1

\*Rsym =  $\sum |F_{\text{obs}}| - |F_{\text{calc}}| / \sum |F_{\text{obs}}|$ , where  $I_0$  = observed intensity and  $\langle I \rangle$  = average intensity obtained from multiple observations of symmetry-related reflections.

‡R factor =  $\sum |F_{\text{obs}}| - |F_{\text{calc}}| / \sum |F_{\text{obs}}|$ . The lower resolution limit of refinement for all structures was 10.0 Å.

§R free =  $\sum |F_{\text{obs}}| - |F_{\text{calc}}| / \sum |F_{\text{obs}}|$ , where all reflections belong to a test set of 10% randomly selected data.

ANO<sub>2</sub>, which has a similarly shaped combining site (37). In addition to the steric complementarity of the binding pocket to the hapten, electrostatic components appear to be crucial for selective binding and orientation. Specifically, at one end of the combining site, a negatively charged patch created by H chain CDR3 residue Asp95 attracts and orients the positively charged trimethylammonium portion of the choline moiety of NPPC (Fig. 3).

**Antibody–Hapten Interactions.** Shape complementarity and electrostatic contributions anchor NPPC in the binding site, allowing for optimal interactions with both H and L chain residues. The absence of water molecules around the ligand contributes to the tight fit in the binding site, and calculations using GRASP (38) reveal that NPPC binding buries 644 Å<sup>2</sup> of combining site surface area from solvent. The contacts from the H chain are provided by just two residues, HCDR2 residue Trp52 and HCDR3 residue Tyr96 (Table III; Fig. 4). Notably, Tyr96 also forms part of a “tyrosine sandwich” involving both itself and LCDR1 residue, Tyr32 (Figs. 3 and 4). These tyrosines play a critical role in binding by effectively encasing the central part of the hapten. HCDR2 residues Trp52 and Met50 combine with residues from LCDR3 (Trp91 and Trp96) to form a hydrophobic well at the base of the binding site that interacts with the choline moiety.

Most of the contacts with NPPC involve hypervariable regions of the M3C65 L chain (Fig. 4; Table III). Asn34

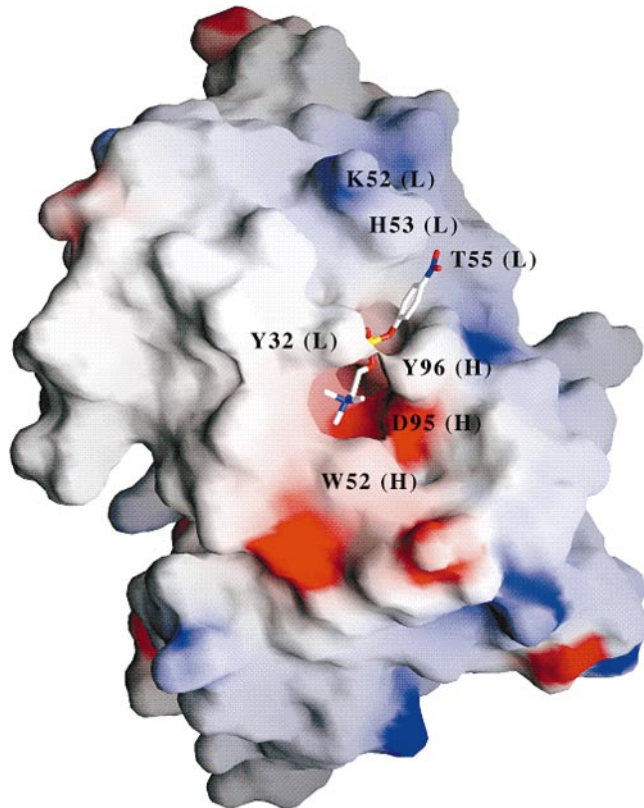


**Figure 3.** The electrostatic surface potential of the M3C65 Fv. Negative and positive potentials are red and blue, respectively, and neutral areas are white. The NPPC hapten is colored by atom type with blue nitrogen, yellow phosphorus, red oxygen, and white carbon. Positions of the three CDR2 L chain mutations (K52, H53, and T55) and other amino acids important in binding NPPC are indicated. The antibody chain designation, H or L, is in parentheses. The figure was generated using GRASP (38).

from LCDR1 hydrogen bonds to O1 of the phosphate group of the hapten, whereas Tyr32, the second half of the “tyrosine sandwich,” encases the phosphate group along with H chain Tyr96. LCDR3 residues Trp91 and Trp96 interact with the choline moiety, completing the aromatic, hydrophobic well at the base of the hapten docking site. There is also a cation–π interaction between the positively charged nitrogen of the choline moiety and the indole ring of Trp96. Cation–π complexes have been shown to be important in other biological systems, including a group I PC-binding antibody M603, where these interactions with aromatic amino acid side chains enhance recognition of choline-containing ligands (39).

LCDR2 is the site of the three mutations at positions 52, 53, and 55 that confer increased binding affinity, and the crystal structure reveals the key roles of His53 and Thr55 in the formation of the combining site. His53 forms two hydrogen bonds, via the side chain Nδ1, to the carbonyls of L chain Gly49 (Nδ1–O, 3.1 Å) and Gly50 (Nδ1–O, 3.1 Å). These hydrogen bonds stabilize the combining site and anchor the side chain of His53 in a position to stack against and interact with NPPC. The side chain of His53 directly

**Table III.** M3C65 Fv Residues in Contact with NPPC

	Segment	Residue	Fv atom	NPPC atom*	Distance
VL	CDR1	Tyr32	C81	C3	3.3
			C $\epsilon$ 1	C3	3.4
			C $\epsilon$ 2	O4	3.2
			C $\delta$ 2	O4	2.8
		Asn34	N82	O1	3.1
	CDR2	His53	N $\epsilon$ 2	O1N	3.4
		Trp91	C $\delta$ 1	C3	3.4
	CDR3		C $\epsilon$ 2	C4	3.4
			C $\eta$ 2	C4	3.4
			C $\zeta$ 2	C4	3.3
			N $\epsilon$ 1	C3	3.3
		Trp96	C $\zeta$ 2	C2	3.8
VH	CDR2	Trp52	C $\eta$ 2	C4	3.3
		Tyr96	C $\delta$ 1	C5A	3.1
	CDR3	C $\epsilon$ 1	C5A	C5A	3.4

\*Labeling of NPPC atoms is shown in Fig. 2 A.

contacts the *p*-nitrophenyl group of NPPC (Table III), and also stacks against its aromatic group. The critical role played by His53 corroborates the finding that CDR2 position 53 is a specificity-determining residue in  $\lambda$  L chains (40).

Residue Thr55 plays two key roles in the architecture of the binding site near the *p*-nitrophenyl group. First, this  $\beta$ -branched residue closes off the end of the binding groove, allowing a tighter fit with the ligand by exclusion of water from the site, which is exposed in antibodies using

the germline L chain. Second, Thr55 engages in a hydrogen bond from the O $\delta$  atom to the carbonyl oxygen of H chain Gly97. This interaction locks the L and H chains together in the specific conformation required for tight binding, and is therefore critical. Notably, this interaction is made possible by the presence of a proline at H chain position 98, which has adopted a cis conformation.

The role of mutated residue Lys52 is less clear, as the side chain is oriented away from the binding pocket. However, comparison of the M3C65 structure to the germline structure suggests that the importance of this mutation may lie in the replacement of the germline asparagine residue. In the germline  $\lambda$ 1 structure, Asn52 hydrogen bonds to Asn53. Such a hydrogen bond would also be possible between germline Asn52 and the mutated M3C65 His53 side chain, a contact that would disrupt the crucial contacts provided by His53. In contrast, a lysine at position 52 would be unlikely to hydrogen bond to His53, allowing His53 to make critical architectural contacts necessary for optimal binding of NPPC. Mutation away from asparagine may be aided by the high mutability index of the germline codon sequence (41).

The structural analyses of several other antibody–hapten interactions indicate that amino acid replacements resulting from somatic mutation may directly affect contact residues, but more frequently elicit their effects indirectly via conformational changes in the binding site (42–46). However, in M3C65, both effects are seen. The His53 and Thr55 replacements, along with the indirect effects of the Lys52 replacement, optimize and fix the shape of the combining cavity, whereas His53 also contacts the hapten directly.

*Comparison of M3C65  $\lambda$ 1 Structure with Germline  $\lambda$ 1.* To assess structural changes in combining site shape resulting from somatic mutation, we compared the M3C65 antibody with that of an unmutated  $\lambda$ 1 structure. Superposi-

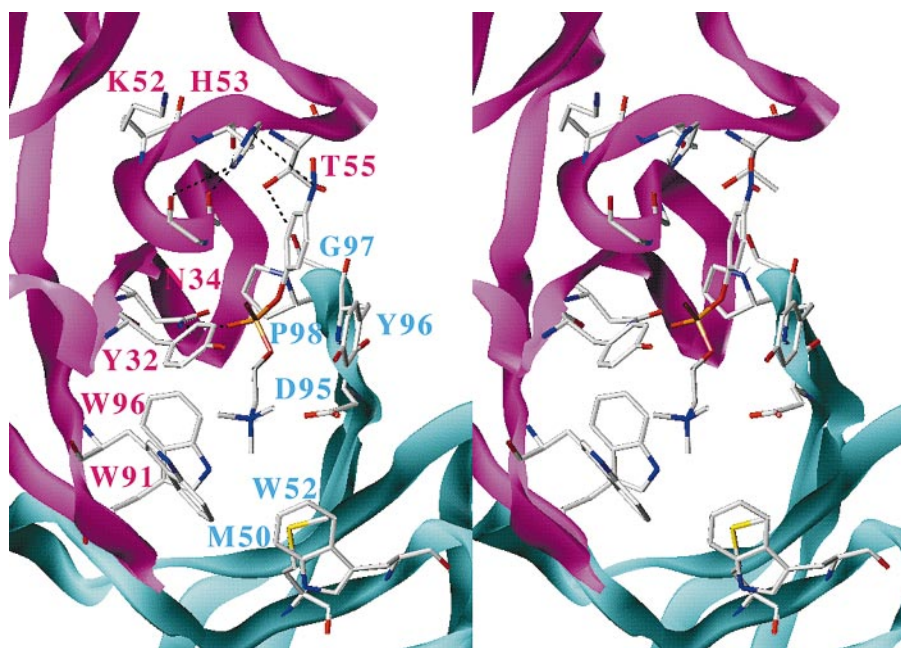


**Figure 4.** Stereo top view of the M3C65 combining site complexed with NPPC, showing residues important for hapten binding. L chain Gly49 and Gly50 are shown in the illustration but are not numbered. The H chain is on the right in blue, and the L chain is on the left in pink. Atom types are indicated by color, with blue nitrogen, gold phosphorus, red oxygen, yellow sulfur, and white carbon. Dashes indicate hydrogen bonds. The figure was generated using SYBYL (Tripos, Inc.).

tioning of hybridoma HC19 germline  $\lambda 1$  (23) with the mutated M3C65 sFv shows that the C $\alpha$  backbone tracings are quite similar, with a root mean square deviation of 0.50 Å for 108 corresponding residues (Fig. 5). Strikingly, the only notable differences between the two structures are observed in LCDR2 and involve residues 52–56, the region containing the mutated residues, with the major shifts occurring in residues Thr55 and Pro56. As noted, this significant shift results from contacts made by the mutated LCDR2 residues His53 and Thr55, thus providing the necessary conformation of the hapten binding pocket. The C $\alpha$  backbone tracings of germline  $\lambda 1$  and M3C65  $\lambda 1$  are very similar. However, one notable shift in amino acid side chain placement occurs in the binding pocket, where L chain residue Tyr32 has rotated  $\sim 90^\circ$  from the germline, orienting the ring face so that it is more perpendicular to the ligand. This rotation of Tyr32 also places the C $\delta$  of Tyr32 closer to the O4 of the ligand phosphate group, a shift from 4.0 to 2.8 Å, such that its positive edge complements the negatively charged phosphate group. This close approach is indicative of an unusually strong C-H $\cdots$ O hydrogen bond (47).

## Discussion

A shift in antibody repertoire occurs after immunization with some hapten–protein conjugates, reflecting recruitment of alternative gene combinations at different stages of the immune response (6). The potential to shift the antibody repertoire could play an important role in determining the ultimate success of immunization, but the molecular forces driving this complex process are not clear. These forces are likely to be multifaceted and may include (a) the precursor frequency of cells expressing a given VH/VL

gene combination (48), (b) intrinsic affinity and/or binding kinetics of the immunoglobulin B cell receptor for ligand (3, 6), (c) adaptability of the immunoglobulin receptor to somatic mutation (8), (d) restrictions in entry into the memory cell compartment because of differences in B cell lineage (49), and (e) idiotypic interactions that may down-regulate dominant clonotypes and promote polyclonality of the developing memory B cell population (6). In addition, as discussed here, competitive advantages may lie in the use of alternative V gene combinations that allow accommodation of carrier structures, resulting in alteration of initial patterns of clonal dominance.

**Repertoire Shift in the Immune Response to PC-KLH.** Immunization of BALB/c mice with PC-KLH leads to expression of two antibody populations differing in fine specificity that predominate in the immune response at different times (7, 12–15). This repertoire shift occurs in the late primary and early secondary response, resulting in loss of initial dominance by antibodies bearing the T15 idiotype (group I) and their replacement by group II antibodies that employ different VH and VL combinations. We propose that the new gene combinations employed by group II antibodies allow recognition of complex PC-carrier epitope(s), and that the ability of these combining sites to be shaped by favorable somatic mutations allows emergence and dominance by group II-specific B cells.

T15 antibodies are restricted to use of the VH1/V $\kappa$ 22 gene combination. These antibodies undergo little affinity maturation (50–53), and mutated T15 antibodies generally have reduced ability to bind antigen (50, 54). It has been suggested that deleterious mutation of primary antibodies contributes to loss of dominance in the memory response (55). However, group II V regions appear to be equally susceptible to harmful

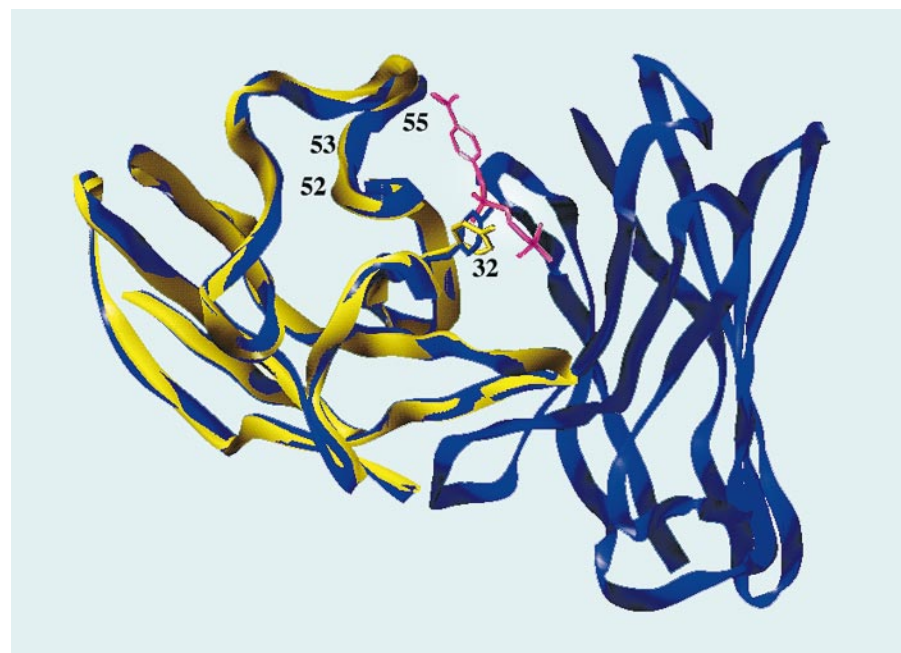


**Figure 5.** Overlay of the M3C65 V region (blue) with the germline  $\lambda 1$  of antibody HC19 (yellow). The orientation of L chain residue Tyr32 is shown for germline  $\lambda 1$  and M3C65. The positions of mutated residues 52, 53, and 55 are indicated. The NPPC hapten (pink) is shown complexed to M3C65. The figure was generated using SYBYL (Tripos, Inc.).

mutations (56, 57). Thus, T15 may be unique in the failure of mutations to improve antigen binding (33).

Group II antibodies use a variety of H and L combinations unrelated to T15 (7). Although the  $\kappa$  L chain is expressed in many memory anti-PC-KLH antibodies,  $\lambda$ -bearing antibodies can dominate (>75%) some responses. To clarify factors conferring selective advantage to these antibodies, we focused on the antigen binding properties and combining site structure of a prototype group II memory antibody, M3C65. We demonstrate that (a) carrier determinants extending from PC contribute to the affinity of M3C65, (b) the shape of the M3C65 combining site is well suited for accommodation of PC in the context of carrier residues, (c) somatic mutation can alter the specificity for carrier determinants, and (d) somatic mutation can increase affinity directly by affecting residues in the combining site that contact ligand and indirectly by modifying the shape of the combining site.

More than 35 years ago, it was suggested that antibodies elicited to conjugated haptens might recognize carrier residues in addition to the haptenic determinant (58). Defining the complete antigenic determinant has been difficult, but in many systems it is thought that the protein carriers of haptens make a significant contribution to binding by anti-hapten antibodies (37, 44, 59). However, T15 has approximately equal intrinsic affinities for PC ( $K_a = 2.9 \times 10^5 \text{ M}^{-1}$ ) and NPPC ( $K_a = 1.8 \times 10^5 \text{ M}^{-1}$ ), indicating the absence of a requirement for the diazophenyl linkage between PC and the protein carrier (60, 61). These results are in agreement with the earlier conclusion that T15 antibodies recognize only the PC portion of DPPC, another hapten that mimics the linkage between PC and protein (13). Thus, the carrier linkage does not appear to be an essential part of the epitope, in contrast to group II antibodies, where the carrier linkage is an essential feature.

**Comparison of Group I and Group II Combining Sites.** Inspection of the binding pockets of two group I antibodies, T15 (43, 62) and the related antibody M603 (63, 64), reveals structural differences that would allow better accommodation of carrier residues by group II antibodies. Fig. 6 shows comparative models of T15 bound to PC and M3C65 bound to NPPC. In the T15 combining site, PC is

bound in a deep pocket anchored by contacts between the antibody and the phosphate group. The cavity of T15 is deeper than M3C65 as a result of longer LCDR1, HCDR2, and HCDR3 loops that protrude farther from the binding pocket. PC occupies only a small portion of the combining site, leaving room for carrier residues; however, the deeper wedge-shaped cavity may hinder accommodation of larger carrier structures. Because of the orientation of PC toward the H chain, the HCDR2 region of T15 would likely interact with carrier epitopes, but the extended length and protrusion of CDR2 may also restrict the carrier interactions by steric hindrance. Although recognition of carrier epitopes can be modulated by mutation of the T15 HCDR2 loop, the effect on binding is subtle (65). The shape of the M3C65 binding site appears to be more suited for binding PC-associated carrier residues than that of T15, and selected mutations may favor such interactions. The elongated shallow groove of the M3C65 combining site provides a flatter surface more akin to antibodies recognizing proteins than the deep pockets of many antibodies recognizing small antigens (18, 46, 66). Extension of carrier residues would continue over the surface of the antibody in such a way as to offer potential interaction with other residues of LCDR2. The more ideal shape of the M3C65 binding site for accommodating carrier compared with T15 is reflected in the 1,000-fold better binding of PC-protein (7, 16). Thus, the basic geometry of the combining sites differs between these two primary and secondary anti-PC antibodies, unlike the response to phenyloxazolone, where it has been postulated that crucial contact residues would maintain the same mode of binding after recruitment of a new VH (67).

**Biological Consequences of Repertoire Shift and Somatic Mutation.** Repertoire shift is commonly observed during immune responses to hapten conjugates, as well as to viral and other protein antigens (55, 68–71). Selective pressure on B cells imposed by affinity for antigen is probably one key factor influencing the changing antibody repertoire (6). In the response to PC-protein, recruitment of new gene combinations produces a corresponding shift away from recognition of free PC toward higher-affinity recognition of PC-protein. The affinity of M3C65 for PC-protein ( $K_a =$

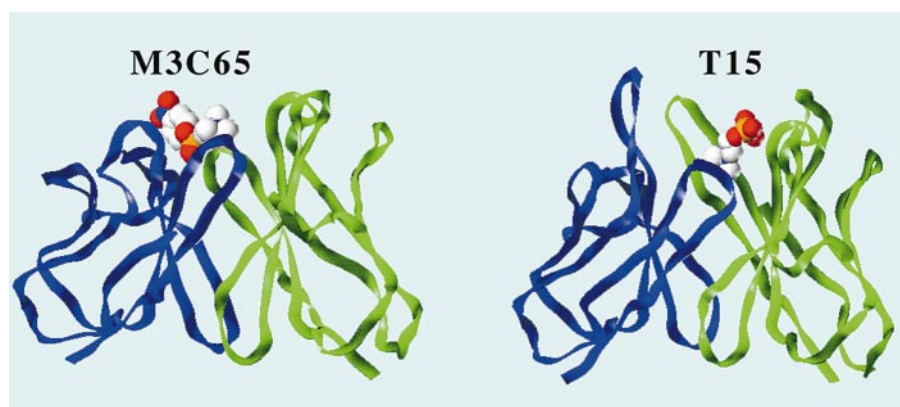


**Figure 6.** Ribbon diagram showing a comparison of the combining sites of M3C65 bound to NPPC (left) and T15 bound to PC (right). The L chain of each antibody is on the left (blue), and the H chain is on the right (green). The figure was generated using SYBYL (Tripos, Inc.).

$1.2 \times 10^8 \text{ M}^{-1}$ ) is in the range for affinities to protein antigens ( $K_a = 10^8\text{--}10^{10} \text{ M}^{-1}$ ) (70, 72, 73), as predicted by Foote and Eisen (74), and as found for a catalytic antibody binding to a hapten-peptide conjugate (46). Moreover, the affinity of the mutated M3C65 for PC-protein is well above the limit for cellular stimulation ( $K_a = 10^6 \text{ M}^{-1}$ ) determined for a monovalent antigen (75). M3C65 expressing germline L chain ( $K_a = 0.5 \times 10^6 \text{ M}^{-1}$ ) is just below this threshold. Presumably, antigen excess and the multivalent nature of PC-KLH allow the repeated selection of germline-encoded group II antibodies in vivo, whereas the acquisition of favorable somatic mutations results in expansion of these antibodies.  $K_a$  values for the various mutants are in the range where differences in affinity affect both the signal transmitted through the B cell receptor and subsequent antigen presentation ( $K_a = 10^6\text{--}10^8 \text{ M}^{-1}$ ), but have not reached the "affinity ceiling" of  $10^{10}$ , beyond which no further benefit occurs (74, 75).

It has been postulated that repertoire shift could be driven by kinetic parameters, such that the hydrophobic and charge characteristics imparted to antibodies by new VH/VL gene combinations provide high association rates leading to more efficient long-range attraction of antigen (3, 76). In addition, a combining site that is more accessible to antigen can lead to faster binding kinetics (48, 77). It will be interesting to determine the kinetic rates of the M3C65 mutant antibodies, as well as those of other group II antibodies, for comparison with the T15 antibody. These comparisons will allow an evaluation of the effect of combining site shape and the consequences of somatic mutation on binding kinetics of antibodies participating in repertoire shift in the anti-PC-KLH response.

The crystal structure of the M3C65 sFv has allowed us to correlate binding with structural features of the antibody that confer advantage to mutated antibodies forming the group II memory pool. The role of somatic mutation in optimizing binding site geometry during affinity maturation has been studied in previous crystallographic analyses of antibody-hapten complexes (44, 67, 78, 79). However, the structural basis of repertoire shift has remained more elusive because of the lack of crystal structures representing different stages of the maturing antibody response. Comparison of T15 and M3C65 binding sites illustrates how the accommodation of carrier residues provides a mechanism for the repertoire shift seen in the immune response to PC-KLH.

We thank J. Morse for help in purifying the sFv protein and Drs. D. Peyton, E. Barbar, and H. Moulton for providing PC coupled to tyrosine, histidine, and tripeptide. We appreciate the critical review of the manuscript by Drs. M. Stenzel-Poore, E. Whitcomb, and T. O'Hare.

This work was supported in part by National Institutes of Health grants AI-14985 and AI-26827 to M.B. Rittenberg and grant GM-49244 to R.G. Brennan. M.A. Schumacher is a 1999 recipient of a Burroughs Wellcome Career Development Award.

Submitted: 18 February 2000

Revised: 25 April 2000

Accepted: 3 May 2000

## References

- Eisen, H.N., and G.W. Siskind. 1964. Variations in affinities of antibodies during the immune response. *Biochemistry*. 3:996–1008.
- Cumano, A., and K. Rajewsky. 1986. Clonal recruitment and somatic mutation in the generation of immunological memory to the hapten NP. *EMBO (Eur. Mol. Biol. Organ.) J.* 5:2459–2468.
- Foote, J., and C. Milstein. 1991. Kinetic maturation of an immune response. *Nature*. 352:530–532.
- Wysocki, L., T. Manser, and M.L. Gefter. 1986. Somatic evolution of variable region structures during an immune response. *Proc. Natl. Acad. Sci. USA*. 83:1847–1851.
- Weigert, M.G., I.M. Cesari, S.J. Yonkovich, and M. Cohn. 1970. Variability in the lambda light chain sequences of mouse antibody. *Nature*. 228:1045–1047.
- Berek, C., and C. Milstein. 1987. Mutation drift and repertoire shift in the maturation of the immune response. *Immunol. Rev.* 96:23–41.
- Stenzel-Poore, M.P., U. Bruderer, and M.B. Rittenberg. 1988. The adaptive potential of the memory response: clonal recruitment and epitope recognition. *Immunol. Rev.* 105: 113–136.
- Manser, T., L.J. Wysocki, T. Gridley, R.I. Near, and M.L. Gefter. 1985. The molecular evolution of the immune response. *Immunol. Today*. 6:94–100.
- Bennett, L., and C.T. Bishop. 1977. Structure of the type XXVII *Streptococcus pneumoniae* (pneumococcal) capsular polysaccharide. *Can. J. Chem.* 55:8–16.
- Lim, P.L., D.T.M. Leung, Y.L. Chui, and C.H. Ma. 1994. Structural analysis of a phosphorylcholine-binding antibody which exhibits a unique carrier specificity for *Trichinella spiralis*. *Mol. Immunol.* 31:1109–1116.
- McWilliam, A.S., G.A. Stewart, and W. Allen. 1986. Phosphorylcholine bearing components of some helminthic parasites: localization to parasite lipoproteins. *Comp. Biochem. Physiol. B*. 85:627–633.
- Chang, S.P., M. Brown, and M.B. Rittenberg. 1982. Immunologic memory to phosphocholine. II. PC-KLH induces two antibody populations that dominate different isotypes. *J. Immunol.* 128:702–706.
- Rodwell, J., P.J. Gearhart, and F. Karush. 1983. Restriction in IgM expression. IV. Affinity analysis of monoclonal anti-phosphorylcholine antibodies. *J. Immunol.* 130:313–316.
- Wicker, L.S., G. Guelde, I. Scher, and J.J. Kenny. 1982. Antibodies from the Lyb5-B cell subset predominate in the secondary IgG response to phosphocholine. *J. Immunol.* 129: 950–953.
- Heusser, C.H., J.P.A. Bews, R. Abersold, and K. Blaser. 1984. Anti-phosphocholine antibodies with a preferred reactivity for either PC or PC phenyl represent independent expressions. *Ann. Immunol.* 135C:123–129.
- Brown, M., M.P. Stenzel-Poore, S. Stevens, S.K. Kondoleon, J. Ng, H.P. Bachinger, and M.B. Rittenberg. 1992. Immunologic memory to phosphocholine keyhole limpet hemocyanin: recurrent mutations in the  $\lambda 1$  light chain increase affinity for antigen. *J. Immunol.* 148:339–346.
- Stenzel-Poore, M.P., and M.B. Rittenberg. 1991. Unequal distribution of replacement mutations in  $\kappa$  and  $\lambda$  light chains and their associated H chains: the group II antibody response to phosphocholine-KLH. In *Somatic Hypermutation*. E.J. Steele, editor. CRC Press, Boca Raton, FL. 95–104.
- Wilson, I.A., and R.L. Stanfield. 1993. Antibody-antigen in-

- teractions. *Curr. Opin. Struct. Biol.* 3:113–118.
19. Boss, M.A., J.H. Kenten, C.R. Wood, and J.S. Emtage. 1984. Assembly of functional antibodies from immunoglobulin heavy and light chains synthesized in *E. Coli*. *Nucleic Acids Res.* 12:3791–3806.
  20. Barbar, E., T.M. Martin, M. Brown, M.B. Rittenberg, and D.H. Peyton. 1996. Binding of phenylphosphocholine-carrier conjugates to the combining site of antibodies maintains a conformation of the hapten. *Biochemistry*. 35:2958–2967.
  21. Moulton, H.M. 1996. Structure and specificity of the binding site of the anti-phenylphosphocholine antibody M3C65: interactions with haptens and hapten-carrier conjugates. Ph.D. thesis. Portland State University, Portland, OR. 197 pp.
  22. Chang, S.P., and M.B. Rittenberg. 1981. Immunologic memory to phosphorylcholine *in vitro*. I. Asymmetric expression of clonal dominance. *J. Immunol.* 126:975–980.
  23. Bizebard, T., Y. Mauguen, J.J. Skehel, and M. Knossow. 1991. Use of molecular replacement in the solution of an immunoglobulin Fab fragment structure. *Acta Crystallogr.* B47: 549–555.
  24. Kissinger, C.R., D.K. Gehlaer, and D.B. Fogel. 1999. Rapid automated molecular replacement by evolutionary search. *Acta Crystallogr.* D55:484–491.
  25. Tronrud, D.E., L.F. TenEyck, and B.W. Matthews. 1985. An efficient general purpose least-squares refinement program for macromolecular structures. *Acta Crystallogr.* A43: 489–501.
  26. Bhat, T.N., G.A. Bently, G. Boulot, M.I. Greene, D. Tello, W. Dall'Acqua, H. Souchon, F.P. Schwarz, R.A. Mariuzza, and R.J. Poljak. 1994. Bound water molecules and conformational stabilization help mediate an antigen-antibody association. *Proc. Natl. Acad. Sci. USA*. 91:1089–1093.
  27. Laskowski, R.A., M.W. MacArthur, and J.M. Thornton. 1993. PROCHECK: a program to check the stereochemical quality of protein structures. *J. Appl. Crystallogr.* 26:283–291.
  28. Gelewitz, E.W., W.L. Riedeman, and I.M. Klotz. 1954. Some quantitative aspects of the reaction of diazonium compounds with serum albumin. *Arch. Biochem. Biophys.* 53:411–423.
  29. Swerdlow, R.D., R.F. Ebert, P. Lee, C. Bonaventura, and K.I. Miller. 1996. Keyhole limpet hemocyanin: structural and functional characterization of two different subunits and multimers. *Comp. Biochem. Physiol.* 113B:537–548.
  30. von Holt, C., W.F. Brandt, H.J. Greyling, G.G. Lindsey, J.D. Retief, J.A. Rodrigues, S. Schwager, and B.T. Sewell. 1989. Isolation and characterization of histones. *Methods Enzymol.* 170:503–522.
  31. Kocks, C., and K. Rajewsky. 1988. Stepwise intraclonal maturation of antibody affinity through somatic hypermutation. *Proc. Natl. Acad. Sci. USA*. 85:8206–8210.
  32. Sharon, J. 1990. Structural correlates of high antibody affinity: Three engineered amino acid substitutions can increase the affinity of an anti-*p*-azophenylarsonate antibody 200-fold. *Proc. Natl. Acad. Sci. USA*. 87:4814–4817.
  33. Chen, C., V.A. Roberts, S. Stevens, M. Brown, M.P. Stenzel-Poore, and M.B. Rittenberg. 1995. Enhancement and destruction of antibody function by somatic mutation: unequal occurrence is controlled by V gene combinatorial associations. *EMBO (Eur. Mol. Biol. Organ.) J.* 14:2784–2794.
  34. Giusti, A.M., N.C. Chien, D.J. Zack, S.-U. Shin, and M.D. Scharff. 1987. Somatic diversification of S107 from an anti-phosphocholine to an anti-DNA autoantibody is due to a single base change in its heavy chain variable region. *Proc. Natl. Acad. Sci. USA*. 84:2926–2930.
  35. Hande, S., and T. Manser. 1997. Single amino acid substitutions in V(H) CDR2 are sufficient to generate or enhance the specificity of two forms of an anti-aronate antibody variable region for DNA. *Mol. Immunol.* 34:1281–1290.
  36. Kussie, P.H., B. Parhami-Seren, L.J. Wysocki, and M.N. Margolies. 1994. A single engineered amino acid substitution changes antibody fine specificity. *J. Immunol.* 152:146–152.
  37. Brünger, A.T., D.J. Leahy, T.R. Hynes, and R.O. Fox. 1991. 2.9 Å resolution structure of an anti-dinitrophenyl-spin-label monoclonal antibody Fab fragment with bound hapten. *J. Mol. Biol.* 221:239–256.
  38. Nicholls, A., K. Sharp, and B.H. Honig. 1991. Protein folding and association: insights from the interfacial and thermodynamic properties of hydrocarbons. *Proteins*. 11:281–296.
  39. Doughtery, D.A. 1996. Cation-π interactions in chemistry and biology: a new view of benzene, Phe, Tyr, and Trp. *Science*. 271:163–168.
  40. Padlan, E.A., C. Abergel, and J.P. Tipper. 1995. Identification of specificity-determining residues in antibodies. *FASEB J.* 9:133–139.
  41. Shapiro, G.S., K. Aviszus, D. Ikle, and L.J. Wysocki. 1999. Predicting regional mutability in antibody V genes based solely on di- and trinucleotide sequence composition. *J. Immunol.* 163:259–268.
  42. Jeffrey, P.D., R.K. Strong, L.C. Sieker, C.Y. Chang, R.L. Campbell, G.A. Petsko, E. Haber, M.N. Margolies, and S. Sheriff. 1993. 26-10 Fab-digoxin complex: affinity and specificity due to surface complementarity. *Proc. Natl. Acad. Sci. USA*. 90:10310–10314.
  43. Chien, N.C., V.A. Roberts, A.M. Giusti, M.D. Scharff, and E.D. Getzoff. 1989. Significant structural and functional change of an antigen-binding site by a distant amino acid substitution: proposal of a structural mechanism. *Proc. Natl. Acad. Sci. USA*. 86:5532–5536.
  44. Strong, R.K., G.A. Petsko, J. Sharon, and M.N. Margolies. 1991. Three-dimensional structure of murine anti-*p*-azophenylarsonate Fab 36-71. 2. Structural basis of hapten binding and idiotype. *Biochemistry*. 30:3749–3757.
  45. Padlan, E.A. 1994. Anatomy of the antibody molecule. *Mol. Immunol.* 31:169–217.
  46. Patten, P.A., N.S. Gray, P.L. Yang, C.B. Marks, G.J. Wedemayer, J.J. Boniface, R.C. Stevens, and P.G. Schultz. 1996. The immunological evolution of catalysis. *Science*. 271:1086–1091.
  47. Derewenda, Z.S., L. Lee, and U. Derewenda. 1995. The occurrence of C-H...O hydrogen bonds in proteins. *J. Mol. Biol.* 252:248–262.
  48. Milstein, C., and M.S. Neuberger. 1996. Maturation of the immune response. *Adv. Protein Chem.* 49:451–485.
  49. Linton, P.J., D. Lo, L. Lai, G.J. Thornbecke, and N.R. Klinman. 1992. Among naive precursor cell subpopulations only progenitors of memory B cells originate germinal centers. *Eur. J. Immunol.* 22:1293–1297.
  50. Gearhart, P.J., N.D. Johnson, R. Douglas, and L. Hood. 1981. IgG antibodies to phosphorylcholine exhibit more diversity than their IgM counterparts. *Nature*. 291:29–34.
  51. Andres, C.M., A. Maddalena, S. Hudak, N.M. Young, and J.L. Claflin. 1981. Anti-phosphocholine hybridoma antibodies II. Functional analysis of binding sites within three antibody families. *J. Exp. Med.* 154:1584–1598.
  52. Claflin, J.L., J. George, C. Dell, and J. Berry. 1989. Patterns of mutations and selection in antibodies to the phosphoch-

- line-specific determinant in *Proteus morganii*. *J. Immunol.* 143: 3054–3063.
53. Chen, C., V.A. Roberts, and M.B. Rittenberg. 1992. Generation and analysis of random point mutations in an antibody CDR2 sequence: many mutated antibodies lose their ability to bind antigen. *J. Exp. Med.* 176:855–866.
54. Clafin, J.L., and J. Berry. 1988. Genetics of the phosphocholine-specific antibody response to *Streptococcus pneumoniae*. *J. Immunol.* 141:4012–4019.
55. Kalinke, U., E.M. Bucher, B. Ernst, A. Oxenius, H.-P. Roost, S. Geley, R. Kofler, R.M. Zinkernagel, and H. Hengartner. 1996. The role of somatic mutation in the generation of the protective humoral immune response against vesicular stomatitis virus. *Immunity*. 5:639–652.
56. Wiens, G.D., K.A. Heldwein, M.P. Stenzel-Poore, and M.B. Rittenberg. 1997. Somatic mutation in VH complementarity-determining region 2 and framework region 2: differential effects on antigen binding and immunoglobulin secretion. *J. Immunol.* 159:1293–1302.
57. Wiens, G.D., V.A. Roberts, E.A. Whitcomb, T. O'Hare, M.P. Stenzel-Poore, and M.B. Rittenberg. 1998. Harmful somatic mutations: lessons from the dark side. *Immunol. Rev.* 162:197–209.
58. Karush, F. 1962. Immunologic specificity and molecular structure. *Adv. Immunol.* 2:1–40.
59. Källberg, E., D. Gray, and T. Leanderson. 1995. The effect of carrier and carrier priming on the kinetics and pattern of somatic mutation in the V $\kappa$ Ox1 gene. *Eur. J. Immunol.* 25: 2349–2354.
60. Bruderer, U., M.P. Stenzel-Poore, H.P. Bachinger, J.H. Fellman, and M.B. Rittenberg. 1989. Antibody combining site heterogeneity within the response to phosphocholine-keyhole limpet hemocyanin. *Mol. Immunol.* 26:63–71.
61. O'Hare, T., and M.B. Rittenberg. 1998. A simple method for determining KAs of both low and high affinity IgG antibodies. *J. Immunol. Methods*. 218:161–167.
62. Brown, M., M.B. Rittenberg, C. Chen, and V.A. Roberts. 1996. Tolerance to single, but not multiple, amino acid replacements in antibody VH CDR2: a means of minimizing B cell wastage from somatic hypermutation? *J. Immunol.* 156: 3285–3291.
63. Segal, D.M., E.A. Padlan, G.H. Cohen, S. Rudikoff, M. Potter, and D.R. Davies. 1974. The three dimensional structure of a phosphorylcholine-binding mouse immunoglobulin Fab and the nature of the antigen binding site. *Proc. Natl. Acad. Sci. USA*. 71:4298–4302.
64. Satow, Y., G.H. Cohen, E.A. Padlan, and D.R. Davies. 1986. Phosphocholine binding immunoglobulin Fab McPC603: an X-ray diffraction study at 2.7 Å. *J. Mol. Biol.* 190:593–604.
65. Brown, M., G.D. Wiens, T. O'Hare, M.P. Stenzel-Poore, and M.B. Rittenberg. 1999. Replacements in the exposed loop of the T15 antibody VH CDR2 affect carrier recognition of PC-containing pathogens. *Mol. Immunol.* 36:205–211.
66. Amit, A.G., R.A. Mariuzza, S.E.V. Phillips, and R.J. Poljak. 1986. Three-dimensional structure of an antigen-antibody complex at 2.8 Å resolution. *Science*. 233:747–753.
67. Alzari, P.M., S. Spinelli, R.A. Mariuzza, G. Boulot, R.J. Poljak, J.M. Jarvis, and C. Milstein. 1990. Three-dimensional structure determination of an anti-2-phenyloxazolone antibody: the role of somatic mutation and heavy/light chain pairing in the maturation of an immune response. *EMBO (Eur. Mol. Biol. Organ.) J.* 9:3807–3814.
68. Berek, C., G.M. Griffiths, and C. Milstein. 1985. Molecular events during maturation of the immune response to oxazolone. *Nature*. 316:412–418.
69. Manser, T., L.J. Wysocki, M.N. Margolies, and M.L. Gefter. 1987. Evolution of antibody variable region structure during the immune response. *Immunol. Rev.* 96:141–162.
70. Newman, M.A., C.R. Mainhart, C.P. Mallett, T.B. Lavoie, and S.J. Smith-Gill. 1992. Patterns of antibody specificity during the BALB/c immune response to hen eggwhite lysozyme. *J. Immunol.* 149:3260–3272.
71. Clarke, S.H., L.M. Staudt, J. Kavalier, D. Schwartz, W.U. Gerhard, and M.G. Weigert. 1990. V region gene usage and somatic mutation in the primary and secondary responses to influenza virus hemagglutinin. *J. Immunol.* 144:2795–2801.
72. Goldbaum, F.A., A. Cauerhoff, A. Velikovsky, A. Llera, M.-M. Riottot, and R.J. Poljak. 1999. Lack of significant differences in association rates and affinities of antibodies from short-term and long-term responses to hen egg lysozyme. *J. Immunol.* 162:6040–6045.
73. Roost, H.P., M.F. Bachmann, A. Haag, U. Kalinke, V. Pliska, H. Hengartner, and R.M. Zinkernagel. 1995. Early high-affinity neutralizing anti-viral IgG responses without further overall improvements of affinity. *Proc. Natl. Acad. Sci. USA*. 92:1257–1261.
74. Foote, J., and H.N. Eisen. 1995. Kinetic and affinity limits on antibodies produced during immune responses. *Proc. Natl. Acad. Sci. USA*. 92:1254–1256.
75. Batista, F.D., and M.S. Neuberger. 1998. Affinity dependence of the B cell response to antigen: a threshold, a ceiling, and the importance of off-rate. *Immunity*. 8:751–759.
76. England, P., R. Nageotte, M. Renard, A.-L. Page, and H. Bedouelle. 1999. Functional characterization of the somatic hypermutation process leading to antibody D1.3, a high affinity antibody directed against lysozyme. *J. Immunol.* 162: 2129–2136.
77. McManus, S., and L. Riechmann. 1991. Use of 2D NMR, protein engineering, and molecular modeling to study the hapten-binding site of an antibody Fv fragment against 2-phenyloxazolone. *Biochemistry*. 30:5851–5857.
78. Lascombe, M.-B., P.M. Alzari, R.J. Poljak, and A. Nisonoff. 1992. Three-dimensional structure of two crystal forms of Fab R19.9 from a monoclonal anti-arsenate antibody. *Proc. Natl. Acad. Sci. USA*. 89:9429–9433.
79. Wedemayer, G.J., P.A. Patten, L.H. Wang, P.G. Schultz, and R.C. Stevens. 1997. Structural insights into the evolution of an antibody combining site. *Science*. 276:1665–1669.
80. Kabat, E.A., T.T. Wu, H.M. Perry, K.S. Gottesman, and C. Foeller. 1991. Sequences of Proteins of Immunological Interest. 5th edition. U.S. Department of Health and Human Services, Bethesda, MD. 2,597 pp.